

# Development of an Excitation and Detection System of Electron Bernstein Waves in LATE

Xingyu GUO, Ryo ASHIDA, Yuto NOGUCHI<sup>1)</sup>, Hitoshi TANAKA, Masaki UCHIDA  
and Takashi MAEKAWA

*Graduate School of Energy Science, Kyoto University, Kyoto 606-8502, Japan*

<sup>1)</sup>*Department of ITER Project, National Institutes for Quantum Science and Technology, 801-1 Mukoyama, Naka-shi, Ibaraki 311-0193, Japan*

(Received 15 November 2021 / Accepted 18 February 2022)

In order to detect the wave pattern of electron Bernstein waves (EBWs), an excitation and detection system has been developed in Low Aspect ratio Torus Experiment (LATE). The system consists of a waveguide launcher with arbitrary polarization, a specially designed five-pin probe antenna, a two-dimensional (2-D) mechanical probe driving system, and a homodyne-type mixer circuit. The excitation and detection system has been tested in the air and shows reliable results.

© 2022 The Japan Society of Plasma Science and Nuclear Fusion Research

Keywords: spherical tokamak, overdense plasma, mode conversion, electron Bernstein wave, direct detection

DOI: 10.1585/pfr.17.1401024

## 1. Introduction

Electron cyclotron waves (ECWs) are widely used in heating and driving currents in fusion plasmas. However, if the plasma is over-dense, i.e., the plasma density is larger than the cutoff density, ECWs will be reflected at the plasma cutoff layer and cannot reach the core region. Electron Bernstein waves (EBWs), generated by a coherent motion of electrons, are a special kind of short-wavelength quasi-electrostatic waves in magnetized hot plasmas. EBWs do not have density limits, express a strong cyclotron damping at all harmonics, and can achieve parallel refractive indices much larger than one. Therefore, they are very suitable for heating and driving currents in high-beta plasmas in various types of magnetic confinement devices such as stellarator or spherical tokamak, in contrast to the conventional electromagnetic waves [1].

Since EBWs do not exist in vacuum and can only be excited inside a magnetized plasma, mode conversion from electromagnetic waves is required for excitation. Three mode conversion methods had been proposed and utilized in a number of experiments: O-X-B [2], high field side launch [3] and X-B [4].

Previous evidence of successful EBWs excitation mainly came from indirect measurements, such as measurements of plasma energy, density, temperature, soft/hard X-ray, electron Bernstein emission (EBE), H- $\alpha$ , stray microwave radiation, etc. Direct measurement of the wave field was only performed in a few experiments. Sugai observed conversion into short-wavelength Bernstein waves near the UHR in a linear machine with a short wire antenna [5]. Podoba *et al.* demonstrated conver-

sion from an O-wave to an X-wave by probe measurements of amplitude and phase of the wave field in the WEGA stellarator [6]. Uchijima *et al.* conducted direct measurement experiments on the mode conversion to EBW in the Mini-RT by three mode-conversion scenarios, but the measured EBW wavelength is about one-order larger than theoretical one [7].

Up to now, there is no direct observation of two-dimensional (2-D) wave pattern in torus configuration. For this reason, an excitation and detection system of EBWs has been developed in Low Aspect ratio Torus Experiment (LATE).

The paper is organized as follows. Section 2 describes the main components of the excitation and detection system. Section 3 presents the cold test results. The summary is given in Sec. 4.

## 2. Excitation and Detection System

The excitation and detection system of EBWs consists of four parts: a waveguide launcher with arbitrary polarization, a specially designed five-pin probe antenna, a 2-D mechanical probe driving system, and a homodyne-type mixer circuit. In this section, each part is described in detail.

### 2.1 Waveguide launcher

In order to excite EBW, the O-X-B method by oblique microwave incidence from the low magnetic field side (outside) is used. 1.5 GHz microwave is generated by an RF power generator, converted to waveguide mode by a waveguide launcher, and eventually, injected into the plasma from the radial port on the mid-plane of LATE for

author's e-mail: guo.xingyu.r19@kyoto-u.jp

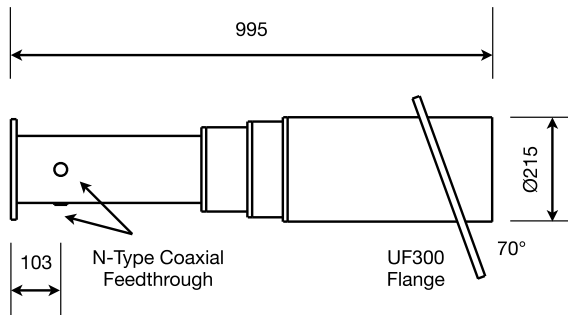


Fig. 1 A schematic diagram of the waveguide launcher. All dimensions are in units millimeter.

EBW excitation.

The launcher is open-end circular waveguide type made of SUS304 with an outer diameter of 215 mm, an inner diameter of 208.3 mm and a total length of 995.7 mm. Two stainless steel rods with a diameter of 7 mm and a length of 44.7 mm are installed inside, in the horizontal ( $x$ ) and vertical ( $y$ ) directions, which are 103.4 mm away from the bottom end. Therefore, a coaxial waveguide converter is formed. A schematic diagram of the waveguide launcher is shown in Fig. 1.

When a high-frequency current flows through the stainless steel rod, the  $TE_{11}$  mode, with the electric field oscillating in the same direction as the rod ( $x, y$  direction), is generated. Arbitrary polarization can be generated by adjusting the relative amplitude and phase of the electric field in the  $x$  and  $y$  directions. In the experiment, a variable attenuator and a phase shifter are used for such adjustment.

The reflectance of the launcher is investigated by using a network analyzer. Measurement results show that the reflection rate in the frequency range of 1.45 to 1.55 GHz used in present experiments is  $-8$  dB (16%) or less.

## 2.2 Five-pin probe antenna

Monopole and dipole antennas used in previous experiments [5–7] are pretty suitable for detecting long-wavelength electromagnetic modes, but not suitable for detecting short-wavelength electrostatic modes. Since the electron temperature of the target plasma generated by LATE is only about several electronvolts in present experiments, the wavelength of EBW is several millimeters. Therefore, a monopole antenna with the antenna chip oriented in the direction of the electric field cannot obtain sufficient spatial resolution for this short-wavelength wave, as the chip length is comparable to the wavelength. To detect EBWs directly, a specially designed five-pin probe antenna is developed.

A schematic diagram of the five-pin probe antenna is shown in Fig. 2. The antenna consists of five mineral-insulated (MI) cables, two ceramic tubes, one stainless steel pipe and one boron nitride (BN) cap.

For the MI cable, the core wire is made of tungsten

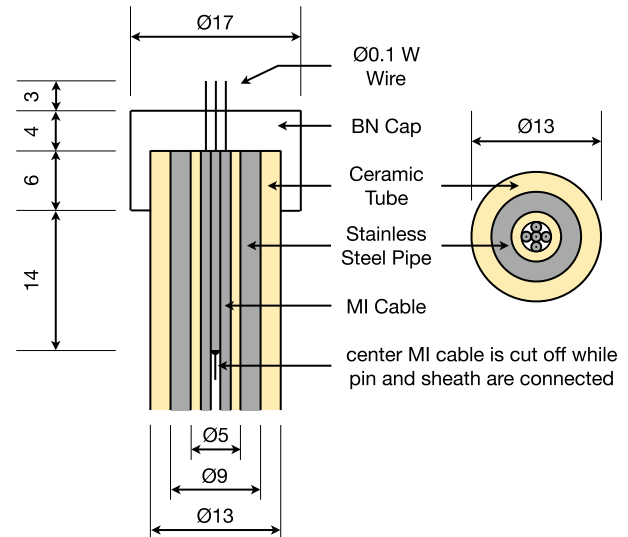


Fig. 2 A schematic diagram of the five-pin probe antenna. All dimensions are in units millimeter.

with a diameter of 0.1 mm, the sheath is made of stainless steel with an outer diameter of 1.14 mm, and the dielectric insulator between them is silicon dioxide ( $SiO_2$ ). The characteristic impedance of the MI cable is  $65 \Omega$ , which is expected to be well matched to the mixer circuit's  $50 \Omega$  impedance. The center MI cable (center pin) is cut off at about 2 cm, and the core wire and sheath are electrically connected by scraping out the insulator from the end and crushing the sheath. By inserting it into the gaps between the four corner MI cables (four corner pins) and making contact with each other, the core wire of the center MI cable and the sheaths of the four corner MI cables are equipotential.

Five pins are guided vertically at the end, fixed and protected by a BN cap (with five holes). The exposed core wire length is 3 mm, and the distance between the center pin and each corner pin is 1 mm.

Five MI cables pass through a ceramic tube for insulation, and outside there is a stainless steel pipe connected to the vacuum vessel, which acts as an electromagnetic shield. And the outermost part is a ceramic tube for protection from the plasma.

The basic idea of the five-pin probe antenna comes from a two-pin antenna method, in which two pins are perpendicular to the electric field and the potential difference between the pins is measured [8]. In principle, a current that is proportional to the potential difference between the center pin and the corner pin is induced in the corner MI cable, therefore, four corner pins can measure electric fields in two orthogonal directions (from the corner pin to the center pin). Since the distance between the center pin and each corner pin is only 1 mm, the antenna is highly sensitive to mm-level short-wavelength modes.

### 2.3 2-D mechanical probe driving system

In the O-X-B method, microwave is injected obliquely with respect to the magnetic field, so it is necessary to measure wave electric field two-dimensionally. In order to perform 2-D measurement of the wave pattern on the mid-plane, a 2-D mechanical probe driving system is developed.

The mechanical system has two rotation axes, which are driven by two stepping motors, respectively. Axis 1 is a hollow-type rotation introduction machine KRP-70 (Kitano Seiki), and axis 2 is a bellows-type rotation introduction machine IRC-70 (Irie Koken). Axis 1 rotates the pulley box itself, while axis 2 rotates the stainless steel pipe and associated antenna box through the belt and pulley in the pulley box. A schematic diagram of the 2-D mechanical probe driving system is shown in Fig. 3.

In order to know the position of the probe antenna, the gear of each axis is attached to a variable resistor, whose resistance depends on the rotation angle. With DC voltage applied to the variable resistor, the rotation angle of each axis and the position of the probe antenna can be easily determined from the voltage change.

It should be mentioned that backlash for axis 1 can be neglected due to tight connection between the pulley box and motor 1, and backlash for axis 2 cannot be neglected as the arm is driven through multiple transmissions. However, such backlash effect can be compensated if extra steps are added when motor 2 reverses direction, and then the arm is rotated back to the zero position. The variable resistor for axis 1 is next to motor 1, while the variable resistor for axis 2 is next to the arm (inside the pulley box, in the

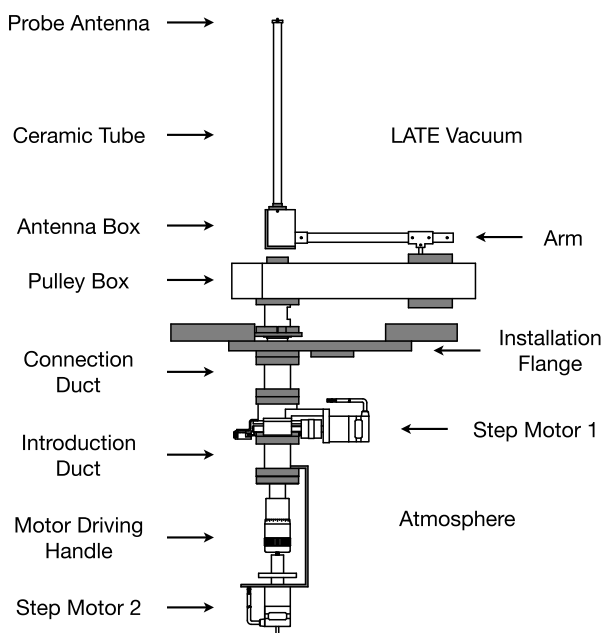


Fig. 3 A schematic diagram of the 2-D mechanical probe driving system (sideview).

vacuum), so both outputs are considered to be accurate.

In the experiment, axis 2 is fixed at a certain value first, while axis 1 is rotated to sweep the antenna during one shot. The sweeping trajectory is shown by a dashed curve in Fig. 4. Then axis 2 is rotated to change the sweeping radius  $R_s$  (the distance between the probe antenna and axis 1 as shown in Fig. 4), and axis 1 is rotated again during next shot. In present experiments, the sweeping radius is in the range of  $R_s = 70$  to 440 mm, and the interval between the sweeps is 10 mm, so there are 38 sweeps in total for one complete 2-D measurement. The measurement area is approximately  $25 \times 30$  cm as shown by the dashed curves in Fig. 4.

It should be noted that the cross on the trajectory in Fig. 4 indicates the relative direction of the five-pin probe antenna, and the direction changes as the antenna moves. This direction is important as it determines the detecting direction of the antenna, and it can be calculated from the rotation angle of axis 1 and 2.

### 2.4 Mixer circuit

Homodyne detection is a useful method of extracting information as phase and amplitude of an oscillating signal, by comparing that signal with a standard oscillation. For direct measurement experiments, a homodyne-type mixer circuit is used to obtain phase and amplitude of the wave pattern. A schematic diagram of the mixer circuit is shown in Fig. 5.

1.5 GHz microwave is generated from the RF oscillator and divided into two parts by the directional coupler, which can be written as

$$V_{RF} = A_{RF} \cos(\omega t + \phi_{RF}). \quad (1)$$

The output part goes to the phase shifter and variable attenuator, and eventually, to the waveguide launcher for EBW

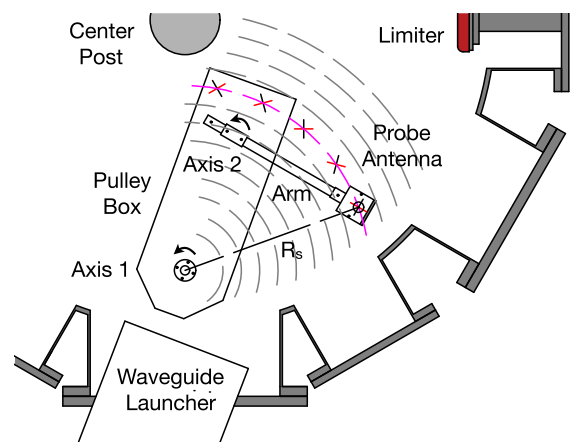


Fig. 4 The measurement area of the 2-D mechanical probe driving system (topview). The sweeping trajectory of the probe antenna during one shot is shown by a dashed curve.

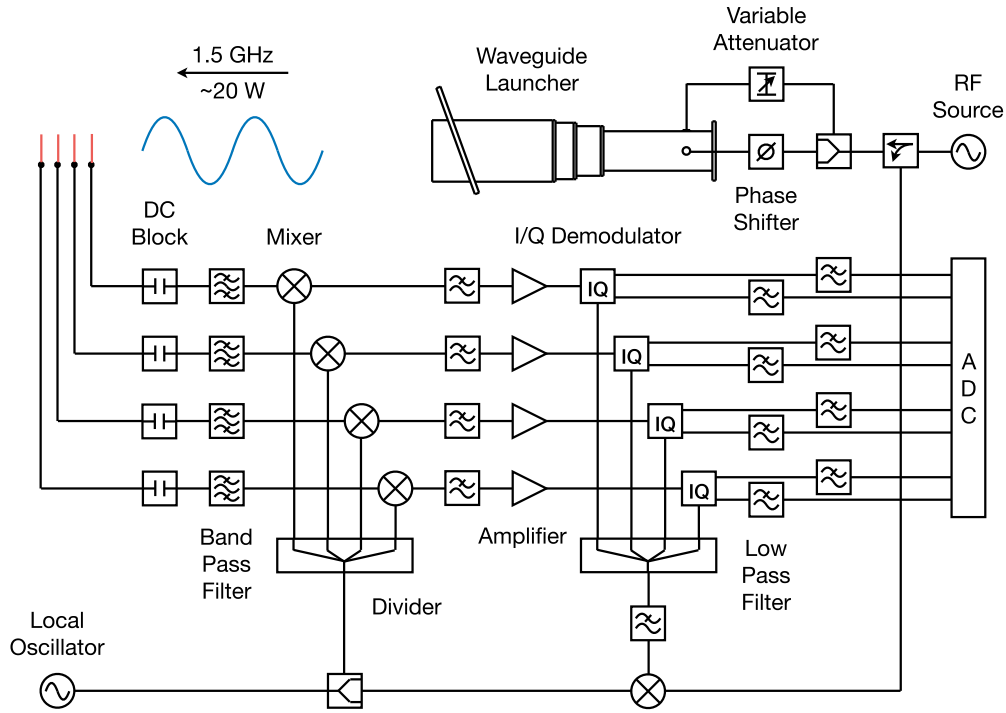


Fig. 5 A schematic diagram of the mixer circuit.

excitation. The coupling part goes to the circuit as a reference 1.5 GHz RF signal.

Detected wave signal from the probe antenna goes to the DC block and band pass filter first, to cut out the large DC voltage from the plasma and keep only 1.5 GHz signal which is of interest. Then this signal,

$$V = A \cos(\omega t + \phi), \quad (2)$$

is mixed with a reference 1.57 GHz LO signal generated from the local oscillator,

$$V_{LO} = A_{LO} \cos[(\omega + \Delta\omega)t + \phi_{LO}]. \quad (3)$$

The mixing signal goes to the low pass filter and amplifier, to keep only 70 MHz signal which contains wave signal information and increase the signal to noise (S/N) ratio, which can be written as

$$V_{70} = AA_{LO} \cos(\Delta\omega t + \phi_{LO} - \phi). \quad (4)$$

Reference 1.5 GHz RF signal and 1.57 GHz LO signal are mixed and low pass filtered so that a reference 70 MHz LO signal is generated as

$$V_{70-Ref} = A_{RF}A_{LO} \cos(\Delta\omega t + \phi_{LO} - \phi_{RF}). \quad (5)$$

These two 70 MHz signals are imported into the in-phase/quadrature-phase ( $I/Q$ ) demodulator, so time-independent sine and cosine signals are exported, as

$$I = A \cos \phi, \quad Q = A \sin \phi. \quad (6)$$

Here constant factors for amplitude and constant shifts for phase are both omitted. Therefore, phase and amplitude information of the wave pattern can be extracted, as

$$\phi = \tan^{-1}(Q/I), \quad A = \sqrt{Q^2 + I^2}. \quad (7)$$

There are four pins in total, and each pin measures phase and amplitude for certain direction and trajectory as shown in Fig. 4. Eight-channel  $I/Q$  outputs go to the analog-to-digital (A/D) converter (NI9215) with a sampling rate of 100 kS/s.

Semi-rigid cables are used for high-frequency signal transmission to suppress losses. The entire circuit is placed inside a shielded box covered with copper mesh to further reduce electromagnetic noises.

The power loss of the band pass filter, mixer, low pass filter,  $I/Q$  demodulator and cables is about 15 dB, the power gain of the amplifier is 25.6 dB, so the total power gain of the circuit is about 10.6 dB. For output amplitude level of about 10 mV, the sensitivity of the circuit is about 3 mV.

### 3. Cold Test Results

In order to verify the reliability of the excitation and detection system, the waveguide launcher and the mixer circuit have been tested in the air. The cold test results are presented in this section.

#### 3.1 Launcher polarization test results

For the waveguide launcher, the electric field in the  $x$

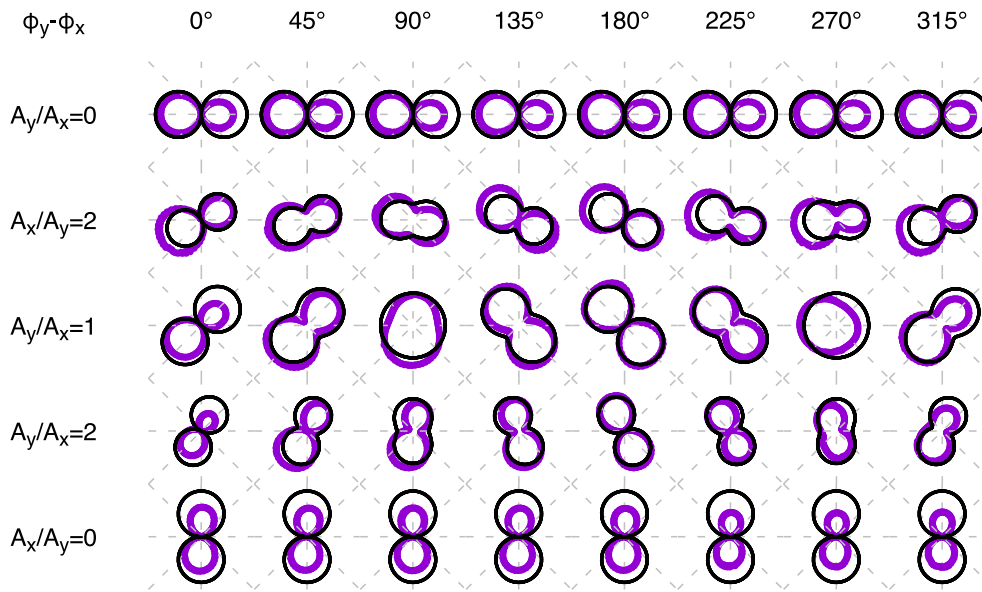


Fig. 6 Waveguide launcher polarization test results. Measured and theoretical results are shown by purple and black curves, respectively.

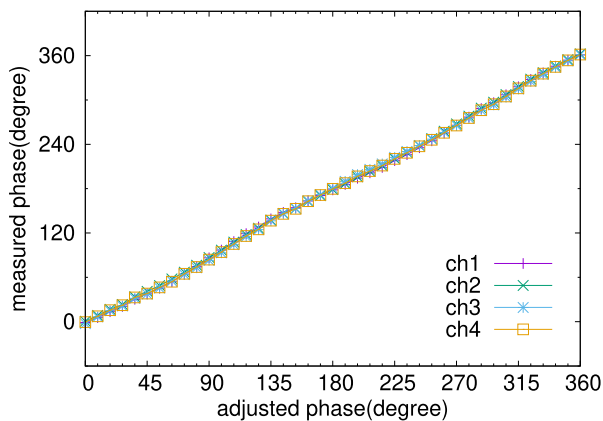


Fig. 7 The relationship between measured phase calculated from output  $I/Q$  signals and adjusted phase from the phase shifter.

and  $y$  directions can be written as

$$E_x = A_x \cos(\phi_x - \omega t), \quad E_y = A_y \cos(\phi_y - \omega t). \quad (8)$$

By adjusting the relative amplitude  $A_x/A_y$  and phase  $\phi_y - \phi_x$ , linear, circular and elliptical polarizations can be generated. The polarization of the waveguide launcher is tested in the air by using a rotating monopole antenna, which is placed at the center position, about 10 cm in front of the launcher. The test results are shown in Fig. 6.

The RF power is fixed at 4 W in the test. Measured results are normalized by linear polarization and fixed antenna direction test results. From Fig. 6, it is noted that theoretical and measured results of the polarization agree relatively well, which means the launcher performance is reliable. The differences between them are partly due to incomplete excitation of the waveguide launcher, and partly

due to inaccurate placement of the monopole antenna (not exactly at the center position and vertical to the horizontal plane).

### 3.2 Mixer circuit test results

To test the mixer circuit, 1.5 GHz microwave is connected with a phase shifter and divided into four parts, which are injected to four channels of the circuit. By adjusting the phase shifter from 0 to 360 degree, variations of eight-channel  $I/Q$  outputs are recorded. Phase of the wave signal can be calculated from output  $I/Q$  signals as  $\phi = \tan^{-1}(Q/I)$ . The relationship between measured phase calculated from output  $I/Q$  signals and adjusted phase from the phase shifter is shown in Fig. 7.

From Fig. 7, it is noted that there is a very good linearity between the measured phase calculated from output  $I/Q$  signals and adjusted phase from the phase shifter, and there is also a good identicalness between four channels.

## 4. Summary

In order to detect the wave pattern of EBWs, an excitation and detection system has been developed in LATE. The system consists of a waveguide launcher with arbitrary polarization, a specially designed five-pin probe antenna, a 2-D mechanical probe driving system, and a homodyne-type mixer circuit.

Cold test results show that the launcher and the circuit performance are pretty reliable. Since the probe antenna is highly sensitive to mm-level short-wavelength modes and the probe driving system can cover a large area on the mid-plane of LATE, the system is ready for direct detection of EBWs.

- [1] H.P. Laqua, Plasma Phys. Control. Fusion **49**, R1 (2007).
- [2] H.P. Laqua *et al.*, Phys. Rev. Lett. **78**, 3467 (1997).
- [3] T. Maekawa *et al.*, Phys. Rev. Lett. **86**, 3783 (2001).
- [4] S. Shiraiwa *et al.*, Phys. Rev. Lett. **96**, 185003 (2006).
- [5] H. Sugai, Phys. Rev. Lett. **47**, 1899 (1981).
- [6] Y.Y. Podoba *et al.*, Phys. Rev. Lett. **98**, 255003 (2007).
- [7] K. Uchijima *et al.*, Plasma Phys. Control. Fusion **57**, 065003 (2015).
- [8] Y.Y. Podoba, *Radio Frequency Heating on the WEGA Stellarator* (PhD Thesis, Ernst-Moritz-Arndt-Universität Greifswald, 2006) p. 64.